M. Campbell

Alternating Gradient Synchrotron Department
Relativistic Heavy Ion Collider Project
BROOKHAVEN NATIONAL LABORATORY
Upton, New York 11973

*Spin Note*

**AGS/RHIC/SN No. 074**

# Field Distriubutions of the Slotted Helical Dipole Prototypes With the Half and Full-Length

Toshiharu Tominaka/ RIKEN

July 22, 1998

# Field Distributions of the Slotted Helical Dipole Prototypes with the Half and Full-Length

T. Tominaka, M. Okamura, and T. Katayama*

The Institute of Physical and Chemical Research (RIKEN), Japan,
*Center for Nuclear Study, School of Science, University of Tokyo, Japan,

July 22, 1998

## 1 INTRODUCTION

The analytically and numerically calculated and measured results of the magnetic field at the center of the slotted helical dipole prototypes with the half and full-length are compared graphically in this report. In addition, the helical multipole fields are also presented, with the comparison for the 2-dimensional (2D) multipoles.

## 2 SLOTTED HELICAL DIPOLE PROTOTYPE WITH THE HALF-LENGTH

The cross section of the slotted helical dipole prototype with the half-length is shown in Fig. 1. Each black dot corresponds to a superconducting strand used as a conductor. The analytically and numerically calculated and measured results of the multipoles are listed in Table 1. The deviation for the intensity of the reference field on the analytical calculation comes from the coil length and relative permeability of the infinity. The measured results are those by the tangential coil.[1] The difference between the calculated and measured results is partly due to a few missing wires occurred on the coil winding stage.[2]

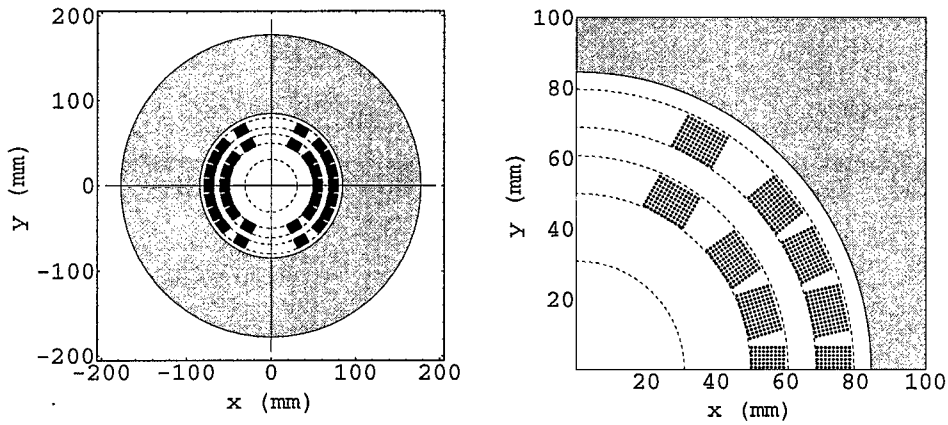


Fig. 1. Cross section of the half-length helical dipole prototype.

Table 1. Helical multipole coefficients ($10^{-4}$) for the half-length helical dipole prototype, at I = 200 A, together with the helical reference field.

| n | Pole | bn (analytical cal.) | bn (TOSCA) | bn / an (measured) | |
|---|---|---|---|---|---|
| (Bref) [T] | | 2.81 | 2.71 | 2.72 | |
| 2 | quadrupole | | | 1.2 | - 0.41 |
| 3 | sextupole | - 49.3 | - 52.4 | - 63.2 | - 0.26 |
| 4 | octupole | | | 2.3 | 0.03 |
| 5 | decapole | 5.5 | 6.0 | 9.7 | 2.4 |
| 6 | dodecapole | | | - 0.54 | - 1.2 |
| 7 | 14 - pole | 0.29 | 0.29 | 3.3 | 7.3 |
| 8 | 16 - pole | | | 0.51 | - 4.0 |
| 9 | 18 - pole | - 7.6 | - 7.8 | - 19.7 | 1.6 |
| 10 | 20 - pole | | | 20.5 | 6.9 |

*2.1 Result of Analytical Calculation*

The magnetic field of the helical dipole can be calculated analytically from the summation for the field contribution of all 1728 (= 864 × 2) turns or 864 sets of four helical line currents with dipole symmetry.[3] In this calculation, the effect of the iron yoke is approximately calculated with the method of image currents, with the assumption of the helical image current similar with the case of the straight current. The relative permeability of iron yoke with the inner diameter of 168.9 mm (= 6.651 inches) is assumed to be infinite. 3D and contour plots of the vertical field component, $B_y$, derived (or synthesized) from the analytical calculation up to 18-pole at I = 200 A, listed in Table 1, are shown in Fig. 2. The required good field region is the interior of the circle of r = 31 mm, shown by the dotted circle in the contour plot of Fig. 2.

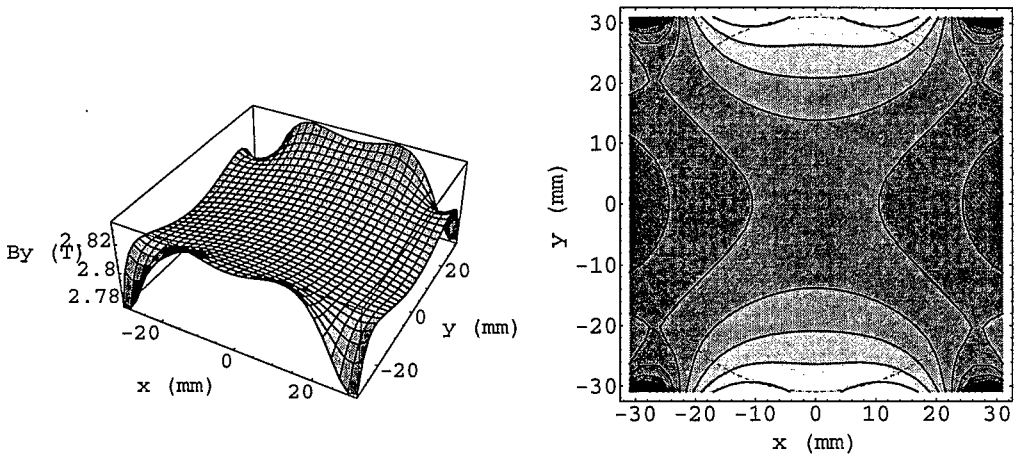


Fig. 2. 3D and contour plots of $B_y$ of the half-length helical dipole with I = 200 A, (analytical calculation).

*2.2 Result of Numerical Calculation*

The magnetic field of the helical dipole is calculated numerically with TOSCA.[4] Numerically calculated 3D and contour plots of $B_y$ of the half-length helical dipole at I = 200 A, are shown in Fig. 3. The multipole contents derived from this field distribution is listed in Table 1

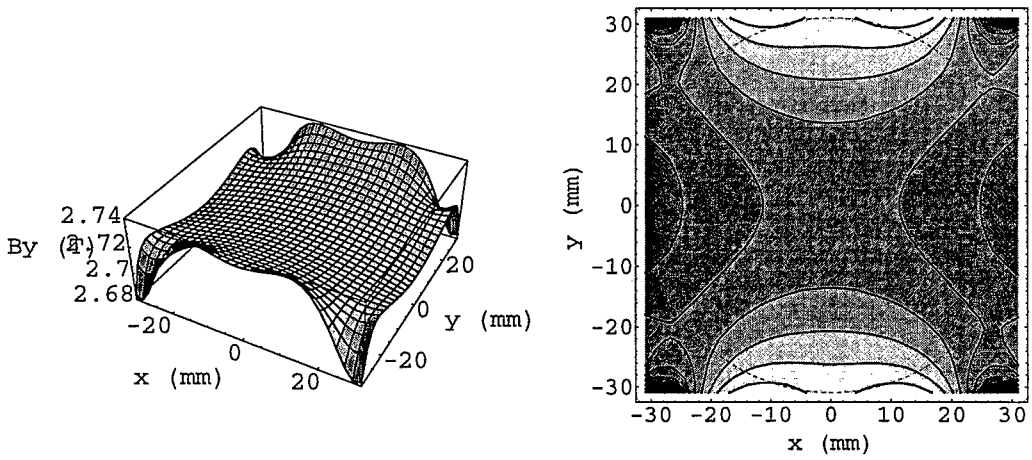


Fig. 3. 3D and contour plots of $B_y$ of the half-length helical dipole prototype at the center with I = 200 A, (TOSCA).

*2.3 Result of Field Measurement*

The magnetic field of the helical dipole was measured by the rotating coil.[1] 3D and contour plots of $B_y$ derived from the measured multipoles up to 20-pole at I = 200 A listed in Table 1, are shown in Fig. 4.

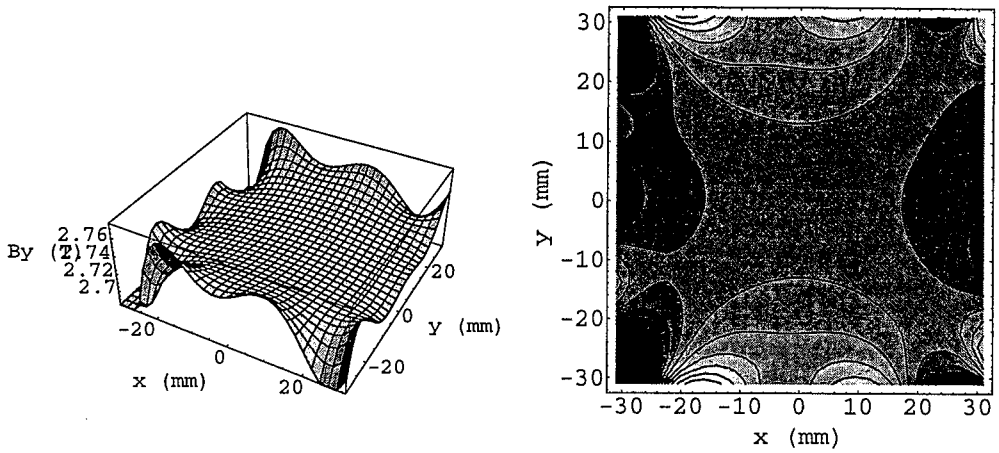


Fig. 4. 3D and contour plots of $B_y$ of the half-length helical dipole prototype with I = 200 A, (measured).

## 3 SLOTTED HELICAL DIPOLE PROTOTYPE WITH THE FULL-LENGTH

The cross section of the slotted helical dipole prototype with the full-length, which is modified or optimized with the removal of the outermost layer from blocks nearest to the pole of the prototype with the half-length, is shown in Fig. 5.

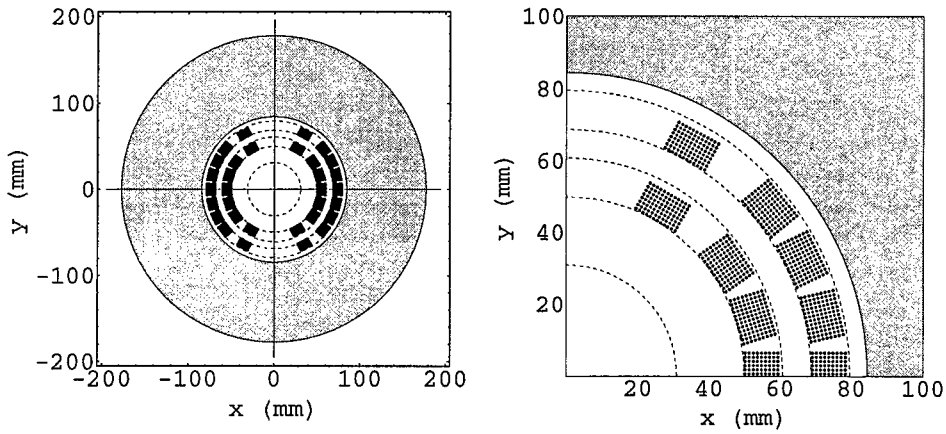


Fig. 5. Cross section of the full-length helical dipole prototype.

Table 2. Helical multipole coefficients ($10^{-4}$) for the full-length helical dipole prototype, together with the transport current and reference field.

| n | Pole | bn (analytical cal.) | bn (TOSCA) | bn (TOSCA) |
|---|---|---|---|---|
| Current [A] | | 300 | 300 | 83 |
| (Bref) [T] | | 4.15 | 3.88 | 1.19 |
| 3 | sextupole | 6.2 | 3.7 | 6.0 |
| 5 | decapole | - 0.34 | - 2.6 | 0.40 |
| 7 | 14 - pole | - 0.84 | - 1.0 | - 0.32 |
| 9 | 18 - pole | - 7.4 | - 8.1 | - 7.1 |

### *3.1 Result of Analytical Calculation*

Analytically calculated 3D and contour plots of $B_y$ of the full-length helical dipole with 840 (= 864 - 24) sets of four helical line currents at I = 300 A, are shown in Fig. 6.

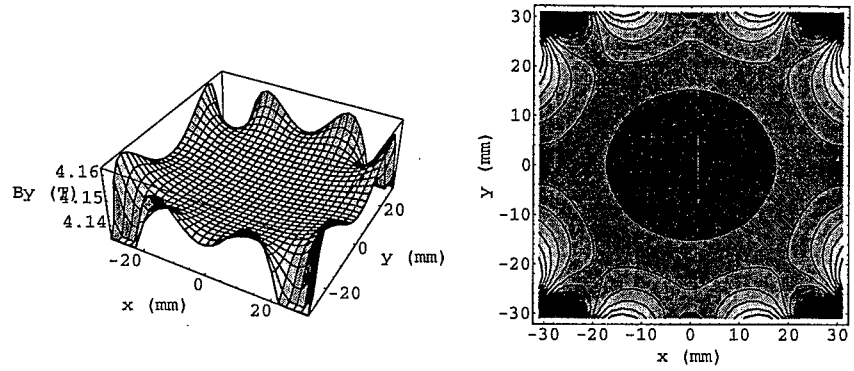


Fig. 6. 3D and contour plots of $B_y$ of the full-length helical dipole prototype with I = 300 A, (analytical calculation).

*3.2 Result of Numerical Calculation*

*3.2.1 At the Low Current of 87 A*

Numerically calculated 3D and contour plots of $B_y$, at I = 87 A, are shown in Fig. 7.

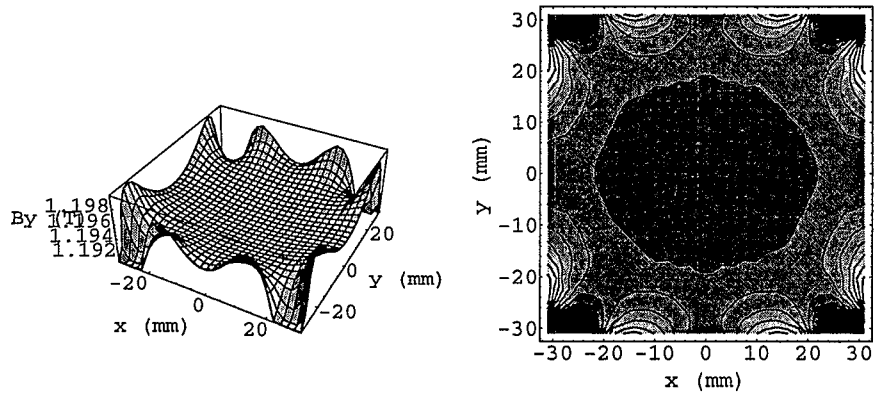


Fig. 7. 3D and contour plots of $B_y$ of the full-length helical dipole prototype at the center with I = 87 A, (TOSCA).

*3.2.2 At the High Current of 300 A*

Numerically calculated 3D and contour plots of $B_y$, at I = 300 A, are shown in Fig. 8.

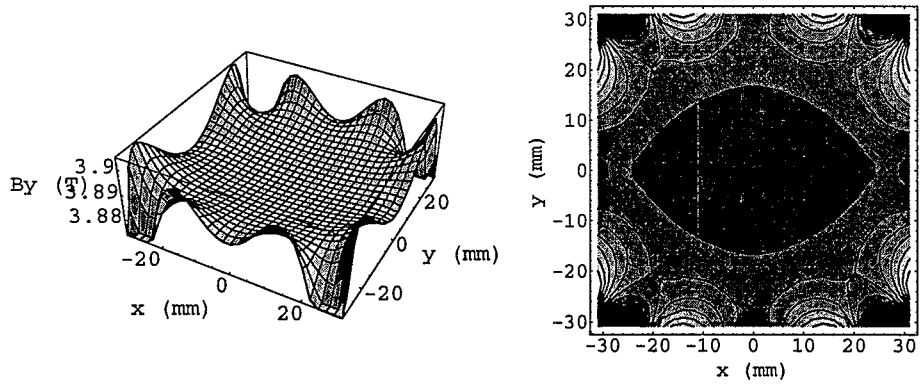


Fig. 8. 3D and contour plots of $B_y$ of the full-length helical dipole prototype at the center with I = 300 A, (TOSCA).

## 4 MULTIPOLE FIELDS

### *4.1 Helical Multipole Fields*

The interior magnetic field of helical dipole coil can be expressed in the following form of the multipole expansion,[5, 6]

$$\begin{cases} B_r(r,\theta,z) = B_{ref}(k)\, r_0 \sum_{n=1}^{\infty} n! \left[\frac{2}{n\,k\,r_0}\right]^n k\, I_n'(n\,k\,r)\left\{-a_n(k)\cos\left(n(\theta - k\,z)\right) + b_n(k)\sin\left(n(\theta - k\,z)\right)\right\} \\ B_\theta(r,\theta,z) = B_{ref}(k)\, r_0 \sum_{n=1}^{\infty} n! \left[\frac{2}{n\,k\,r_0}\right]^n \frac{I_n(n\,k\,r)}{r}\left\{a_n(k)\sin\left(n(\theta - k\,z)\right) + b_n(k)\cos\left(n(\theta - k\,z)\right)\right\} \\ B_z(r,\theta,z) = B_{ref}(k)\, r_0 \sum_{n=1}^{\infty} (-k)\, n! \left[\frac{2}{n\,k\,r_0}\right]^n I_n(n\,k\,r)\left\{a_n(k)\sin\left(n(\theta - k\,z)\right) + b_n(k)\cos\left(n(\theta - k\,z)\right)\right\} \end{cases} \quad (1)$$

where $k = 2\pi/L$ is a twist pitch, L is the length of the $2\pi$ rotation, and $B_{ref}(k)$ is the (k dependent) reference field, which is the transverse field at the beam axis, $B_{ref}(k) = B_y(r=0)$. As a result, the distribution of the y-directional transverse field, $B_y$, can be also expressed as follows,

$$B_y(r,\theta,z=0) = B_{ref}(k) \sum_{n=1,3,5}^{\infty} b_n(k)\, r_0\, n! \left[\frac{2}{n\,k\,r_0}\right]^n \left\{k\, I_n'(n\,k\,r)\sin n\theta \sin\theta + \frac{I_n(n\,k\,r)}{r}\cos n\theta \cos\theta\right\}$$

$$= B_{ref}(k) \sum_{n=1,3,5,..}^{\infty} b_n(k)\, M_n(k,r,\theta) \quad (2)$$

where

$$M_n(k,r,\theta) = r_0\, n! \left[\frac{2}{n\,k\,r_0}\right]^n \left\{k\, I_n'(n\,k\,r)\sin n\theta \sin\theta + \frac{I_n(n\,k\,r)}{r}\cos n\theta \cos\theta\right\} \quad (3)$$

The helical multipole fields for $B_y$, $M_n(k,r,\theta)$ for n = 1, 3, 5, ..., are plotted in Figs. 9 - 13, for k = $2\pi/2.4$ (rad/m), and $r_0$ = 31 mm. The magnetic field of the helical dipole as shown in Figs. 2 - 4 and 6 - 8 is the superposition of the helical multipole fields shown in Figs. 9 - 13.

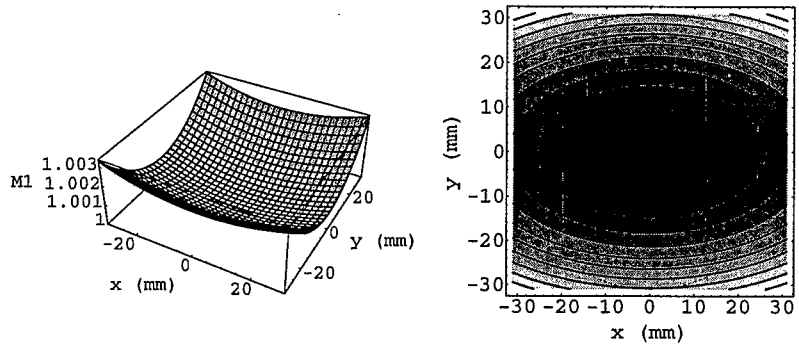


Fig. 9. 3D and contour plots of the helical dipole field, $M_1(k,r,\theta)$, for $B_y$.

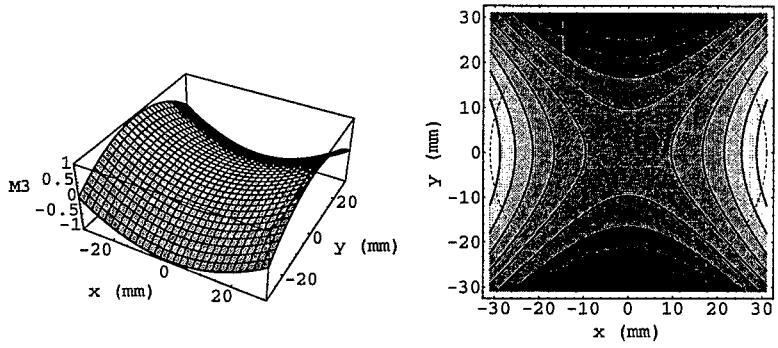


Fig. 10. 3D and contour plots of the helical sextupole field, $M_3(k,r,\theta)$, for $B_y$.

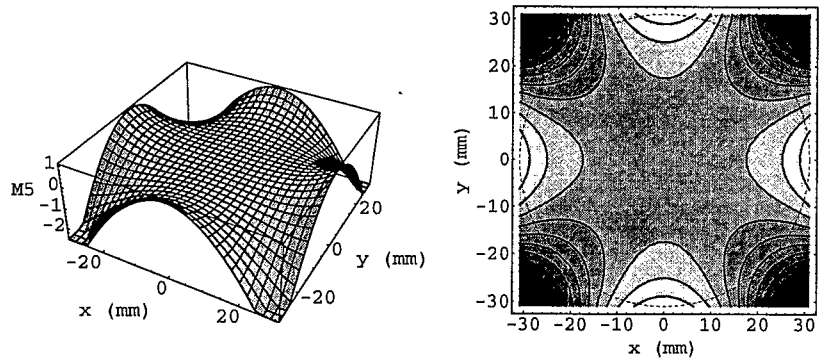


Fig. 11. 3D and contour plots of the helical decapole field, $M_5(k,r,\theta)$, for $B_y$.

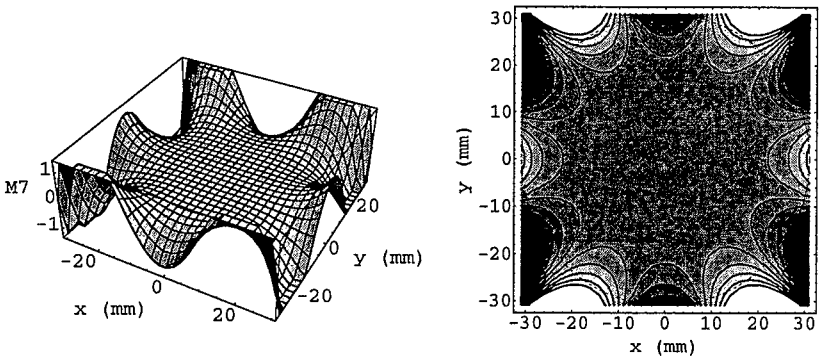


Fig. 12. 3D and contour plots of the helical 14-pole field, $M_7(k,r,\theta)$, for $B_y$.

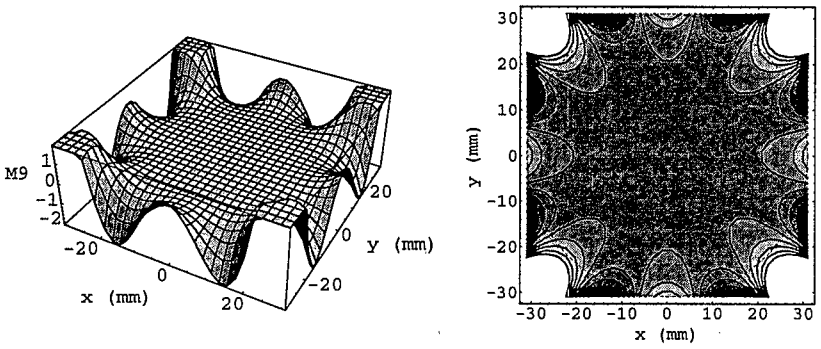


Fig. 13. 3D and contour plots of the helical 18-pole field, $M_9(k,r,\theta)$, for $B_y$.

### *4.2 Comparison with 2D Multipole Fields*

Generally, the magnetic field of 2D or straight dipole magnet can be expressed as the multipole expansion,

$$\begin{cases} B_r(r,\theta) = B_{ref} \sum_{n=1}^{\infty} \left[\frac{r}{r_0}\right]^{n-1} \left\{-a_n \cos n\theta + b_n \sin n\theta\right\} \\ B_\theta(r,\theta) = B_{ref} \sum_{n=1}^{\infty} \left[\frac{r}{r_0}\right]^{n-1} \left\{a_n \sin n\theta + b_n \cos n\theta\right\} \end{cases} \quad (4)$$

Then, it results that the asymptotic form for $k \to 0$ ($L \to \infty$) of $B_{y,\,helix}(r,\theta,z=0)$ of Eq.(2) for helical dipole magnets is equal to $B_{y,\,2d}(r,\theta,z=0)$ for 2-dimensional dipole magnets,

$$\lim_{k\to 0}\left[B_{y,helix}(r,\theta,z=0)\right] = B_{y,2d}(r,\theta) = B_{ref}\sum_{n=1,3,5,..}^{\infty} b_n \left(\frac{r}{r_0}\right)^{n-1}\cos\left[(n-1)\theta\right] \tag{5}$$

The angular dependence for the helical multipole components, $M_n(k)$ for n = 1, 3 and 5 at $r = r_0$ (=31 mm) are shown in Figs. 14 - 16 for three different twist pitch of k = 0, $2\pi/2.4$ and $2\pi/2.4 \times 5$ [rad/m].

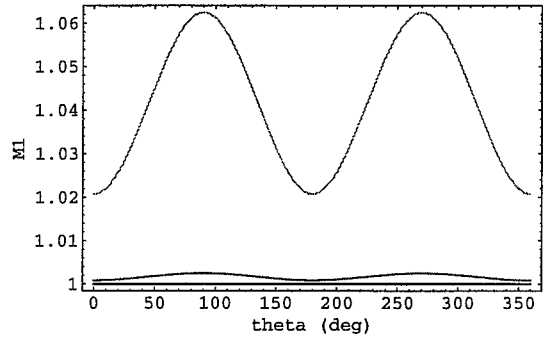


Fig. 14. Angular dependence of the helical dipole component, $M_1(k)$, at $r = r_0 = 31$ mm for k = 0 (black), $2\pi/2.4$ (dark gray), and $2\pi/2.4 \times 5$ [rad/m] (light gray).

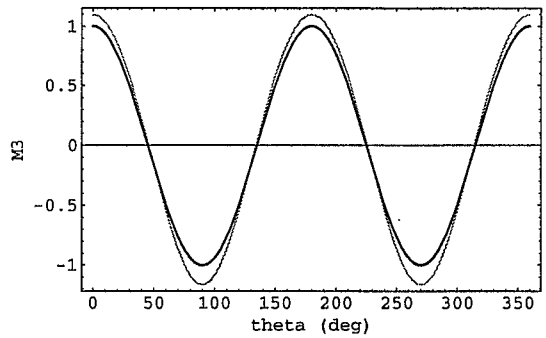


Fig. 15. Angular dependence of the helical sextupole component, $M_3(k)$, at $r = r_0 = 31$ mm for k = 0 (black), $2\pi/2.4$ (dark gray), and $2\pi/2.4 \times 5$ [rad/m] (light gray).

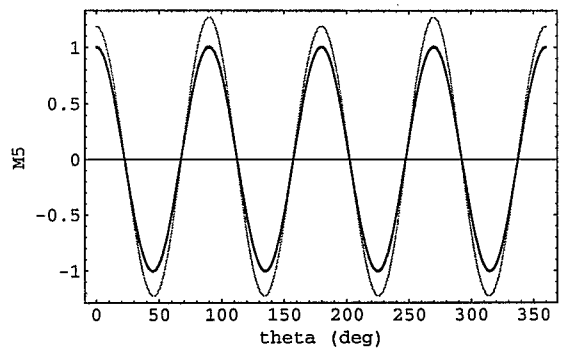


Fig. 16. Angular dependence of the helical decapole component, $M_5(k)$, at $r = r_0 = 31$ mm for k = 0 (black), $2\pi/2.4$ (dark gray), and $2\pi/2.4 \times 5$ [rad/m] (light gray).

In Figs. 15 and 16, two plots for k = 0 and $2\pi/2.4$ are almost same. It is realized that the major difference between the helical and 2D dipole magnets comes from dipole component with $b_1 = 1$ for the small higher multipole coefficients of $b_n = O(10^{-4})$. In order to get the circular homogeneous region for $B_y$, $8.2 \times 10^{-4}$ is the most favorable as the helical sextupole coefficient, for $k = 2\pi/2.4$ (rad/m).[6] It comes from the compensation with the helical sextupole for the non uniform distribution of the helical dipole component.

## 5 CONCLUSION

The analytically and numerically calculated and measured field distribution for the slotted helical dipole magnets with the half and full-length are compared graphically with good agreement. It is also realized that the field distribution is expressed by the superposition of the helical multipole fields deformed from the 2D fields. In addition, it seems that the multipole contents up to 20-pole is needed for the description of the interior field within r = 31 mm for the slotted helical dipole prototype with the full-length.

## 6 ACKNOWLEDGMENTS

The authors are indebted for providing the experimental data and helpful discussions and comments to A. Jain, R. Thomas, and E. Willen.

## REFERENCES

[1] T. Tominaka, "Data Analysis of the Magnetic Field Measurement of a Helical Dipole Prototype Magnet by the Rotating Coil", AGS/RHIC/SN No.65, September 22, (1997).
[2] E. Willen, Private communications.
[3] T. Tominaka, "Analytical Field Calculation of the Slotted Helical Dipole", AGS/RHIC/SN No.47, November 12, (1996).
[4] M. Okamura, "Multipole Components in the BNL Type Helical Dipole Magnet", AGS/RHIC/SN No.46, November 12, (1996).
[5] T. Tominaka et al., "Analytical Field Calculation of the Helical Dipole Magnets for RHIC", Proc. of 1997 Particle Accelerator Conference, to be published.
[6] T. Tominaka et al., "Intrinsic Limits of Field Homogeneity of Helical Dipoles", Proc. of 1998 Asian Particle Accelerator Conference, to be published.

**RIKEN Accelerator Research Facility**
RIKEN (*The Institute of Physical and Chemical Research*)
Hirosawa 2-1, Wako-shi, Saitama 351-0106
Japan

Tel 81 48 462 1111
Telefax 81 48 461 5301
Telex 2962818 RIKEN J

**Dated:** July 22, 1998

Ms. Mary Campbell
Bldg. 911B
Brookhaven National Laboratory
PO Box 5000;
Upton, NY 11973-5000
U.S.A.

Dear Mary:

Enclosed is my report, which I would like to submit for Spin Note.

1) Field Distributions of the Slotted Helical Dipole Prototypes with the Half and Full-Length

Sincerely yours,

Toshi Tominaka

Toshiharu Tominaka
Cyclotron Laboratory
RIKEN
E-mail : tominaka@postman.riken.go.jp

Enclosure

**RIKEN Accelerator Research Facility**
RIKEN (*The Institute of Physical and Chemical Research*)
Hirosawa 2-1, Wako-shi, Saitama 351-0106
Japan

Tel 81 48 462 1111
Telefax 81 48 461 5301
Telex 2962818 RIKEN J

---

**Dated:** July 22, 1998

Ms. Mary Campbell
Bldg. 911B
Brookhaven National Laboratory
PO Box 5000;
Upton, NY 11973-5000
U.S.A.

DIST

Dear Mary:

Enclosed is my report, which I would like to submit for Spin Note.

1) Field Distributions of the Slotted Helical Dipole Prototypes with the Half and Full-Length

Sincerely yours,

Toshi Tominaka

Toshiharu Tominaka
Cyclotron Laboratory
RIKEN
E-mail : tominaka@postman.riken.go.jp

Enclosure